Quantum Voting Machine Encoded with Microwave Photons

Yu Zhang(张钰)[1,2,3*], Chuiping Yang(杨垂平)[4], Qiping Su(苏奇平)[4], Yihao Kang(康逸豪)[4], Wen Zheng(郑文)[1,2,3], Shaoxiong Li(李邵雄)[1,2,3], and Yang Yu(于扬)[1,2,3,5*]

[1]*National Laboratory of Solid State Microstructures, School of Physics, Nanjing University, Nanjing 210093, China*
[2]*Shishan Laboratory, Nanjing University, Suzhou 215163, China*
[3]*Synergetic Innovation Center of Quantum Information and Quantum Physics, University of Science and Technology of China, Hefei 230026, China*
[4]*Department of Physics, Hangzhou Normal University, Hangzhou 310036, China*
[5]*Hefei National Laboratory, Hefei 230088, China*

(Received 7 May 2024; accepted manuscript online 19 June 2024)

We propose a simple quantum voting machine using microwave photon qubit encoding, based on a setup comprising multiple microwave cavities and a coupled superconducting flux qutrit. This approach primarily relies on a multi-control single-target quantum phase gate. The scheme offers operational simplicity, requiring only a single step, while ensuring verifiability through the measurement of a single qubit phase information to obtain the voting results. It provides voter anonymity, as the voting outcome is solely tied to the total number of affirmative votes. Our quantum voting machine also has scalability in terms of the number of voters. Additionally, the physical realization of the quantum voting machine is general and not limited to circuit quantum electrodynamics. Quantum voting machine can be implemented as long as the multi-control single-phase quantum phase gate is realized in other physical systems. Numerical simulations indicate the feasibility of this quantum voting machine within the current quantum technology.

DOI: 10.1088/0256-307X/41/7/070302

The voting machine is a common decision-making tool widely used by various groups to vote on specific proposals. Generally, as long as it receives more than a certain proportion (usually 50%) of the votes, the proposal can be passed and implemented. It is an indispensable tool in group decision making. Anonymity and verifiability of the voting results are fundamental requirements for the voting machine. Recently, some quantum voting schemes have been proposed.[1–5] A novel quantum voting protocol using single-particle states was proposed to select multiple winners securely against malicious attacks.[1] A quantum voting protocol using non-orthogonal coherent states was proposed, eliminating the need for quantum memory storage.[2] A quantum voting scheme was proposed based on locally indistinguishable orthogonal product states for efficient voting systems.[3] A simple quantum voting scheme[4] based on multi-particle entangled states was reported, it is suitable for large scale general votings and provides a proof of security against the most general type of attack. The proposed quantum voting protocol[5] ensures anonymity through the use of quantum operations and the chinese remainder theorem, making it infeasible for attackers to extract private information from partial qubits. However, a quantum voting machine (QVM) has not yet been implemented in circuit quantum electrodynamics (QED). In this Letter, we propose a QVM based on circuit QED with microwave photon qubit encoding.

Circuit QED, formed through the integration of microwave cavities and superconducting (SC) qubits, has emerged as one of the leading candidates for quantum information processing.[6–9] After more than two decades of development, the coherence time of SC qubits has significantly improved from the initial nanosecond scale to hundreds of microseconds[10,11] or even surpassing one millisecond.[12,13] Furthermore, experiments have revealed the existence of one-dimensional microwave resonators characterized by a high quality factor ($Q \gtrsim 10^6$),[14–19] as well as three-dimensional microwave cavities with a high quality factor ($Q \gtrsim 3.5 \times 10^7$).[20–22] The experimental validation of these high quality factors suggests that microwave cavities or resonators contain microwave photons with lifetimes similar to those of SC qubits.[23] The utilization of microwave fields and photons for quantum state engineering and quantum information processing has garnered considerable recent interest.[24–32]

As depicted in Fig. 1, the function of the QVM is to determine the total number of voters in favor of the event being voted upon at the conclusion of the voting process. In Fig. 1(a), the voters can be denoted as $|C_1C_2C_3\cdots C_N\rangle$, where $C_1, \ldots, C_N \in \{0, 1\}$, and the state $|1\rangle$ represents affirmative vote, while the state $|0\rangle$ represents negative vote. The event being voted upon can be denoted as $|X\rangle$. As shown in Fig. 1(b), when X is 0, the quantum state of the system remains unchanged. When X is 1, the sys-

*Corresponding authors. Email: smutnauq@nju.edu.cn; yuyang@nju.edu.cn
© 2024 Chinese Physical Society and IOP Publishing Ltd

tem's quantum state acquires a phase related to the state of each voter. The function of QVM is given by the following equation:

$$U|C_1, C_2, \ldots, C_N, 0\rangle = |C_1, C_2, \ldots, C_N, 0\rangle,$$
$$U|C_1, C_2, \ldots, C_N, 1\rangle = e^{i\frac{\pi\sum_{l=1}^{N} C_l}{N}}|C_1, C_2, \ldots, C_N, 1\rangle, \quad (1)$$

where U is actually a multi-control single-target quantum phase gate. We implement this QVM based on such a device, multiple microwave cavities coupled to a common flux qutrit [Fig. 2(a)]. The N microwave cavities on the left represent N voters, while the one on the right represents the event to be voted on. The three levels of the qutrit are labeled as $|g\rangle$, $|e\rangle$, and $|f\rangle$ [Fig. 2(b)]. Suppose that cavity l ($l = 1, 2, \ldots, N$) are dispersively coupled to the $|g\rangle \leftrightarrow |f\rangle$ transition with coupling constant g_l and detuning δ_l but highly detuned (decoupled) from the $|e\rangle \leftrightarrow |f\rangle$ transition of the qutrit. In addition, assume that cavity x is dispersively coupled to the $|e\rangle \leftrightarrow |f\rangle$ transition with coupling constant g_x and detuning δ_x but highly detuned (decoupled) from the $|g\rangle \leftrightarrow |f\rangle$ transition of the qutrit [Fig. 2(b)]. These conditions can be met by prior adjustment of the level spacings of the qutrit or the frequencies of the cavities. Note that both of the level spacings of an SC qutrit and the frequency of a microwave cavity can be rapidly tuned within a few nanoseconds.[33–35]

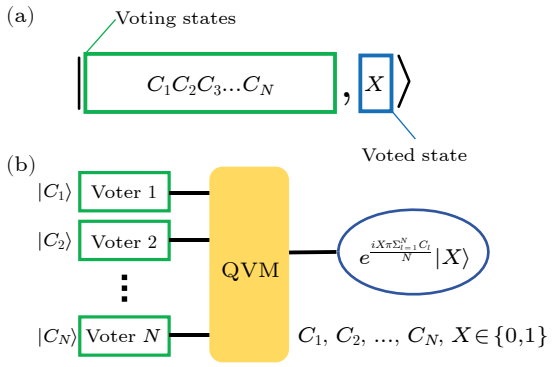

Fig. 1. Schematic diagram illustrating the function of the QVM. (a) The composition of quantum state used in the QVM. (b) When $X = 1$, a phase related to the total number of affirmative votes is introduced into the quantum state.

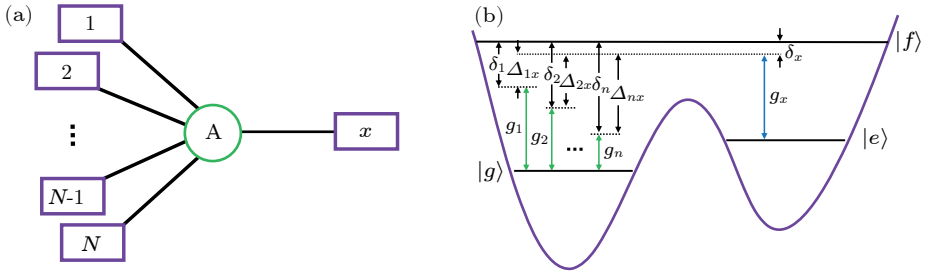

Fig. 2. (a) Schematic circuit of $N + 1$ microwave cavities coupled to a common flux qutrit. Each purple box represents a microwave cavity. The circle A represents the flux qutrit, which is inductively or capacitively coupled to each cavity. (b) Level configuration of the flux qutrit, for which the transition between the two lowest levels can be made weak by increasing the barrier between two potential wells.

After the above considerations, the Hamiltonian of the whole system in the interaction picture and under the rotating wave approximation is given by (assuming $\hbar = 1$)

$$H_I = \sum_{l=1}^{N}\left(g_l e^{-i\delta_l t}\hat{a}_l^{+}\delta_{fg}^{-} + \text{H.c.}\right) + g_x e^{-i\delta_x t}\hat{a}_x^{+}\delta_{fe}^{-} + \text{H.c.}, \quad (2)$$

where $\hat{a}_l$ ($\hat{a}_x$) is the photon annihilation operator of cavity l (cavity x), $\sigma_{fg}^{-} = |g\rangle\langle f|$, $\sigma_{fe}^{-} = |e\rangle\langle f|$, $\delta_l = \omega_{fg} - \omega_{c_l} > 0$, and $\delta_x = \omega_{fe} - \omega_{c_x} > 0$ [Fig. 2(b)]. Here, ω_{fg} (ω_{fe}) is the $|f\rangle \leftrightarrow |g\rangle$ ($|f\rangle \leftrightarrow |e\rangle$) transition frequency of the qutrit, while ω_{c_l} (ω_{c_x}) is the frequency of cavity l (x).

Under the large detuning conditions $\delta_l \gg g_l$ ($l = 1, 2, 3, \ldots, N$) and $\delta_x \gg g_x$, the energy exchange between the coupler qutrit and the cavities is negligible. In addition, under the condition of

$$\frac{|\delta_l - \delta_{l'}|}{\delta_l^{-1} + \delta_{l'}^{-1}} \gg g_l g_{l'}, \quad (3)$$

(where l, $l' \in \{1, 2, \ldots, N\}$ and $l \neq l'$), the interaction between the cavities $(1, 2, \ldots, N)$, induced by the coupler qutrit, is negligible. Therefore, Hamiltonian (2) becomes[36–38]

$$H_e = \sum_{l=1}^{N}(-\lambda_l\hat{n}_l|g\rangle\langle g| + \lambda_l(1+\hat{n}_l)|f\rangle\langle f|) - \lambda_x\hat{n}_x|e\rangle\langle e| + \lambda_x(1+\hat{n}_x)|f\rangle\langle f| - \sum_{l=1}^{N}\lambda_{lx}(e^{i\Delta_{lx}t}\hat{a}_l\hat{a}_x^{+}\sigma_{ge}^{-} + \text{H.c.}), \quad (4)$$

where $\sigma_{eg}^{-} = |g\rangle\langle e|$, $\lambda_l = g_l^2/\delta_l$, $\lambda_x = g_x^2/\delta_x$, $\lambda_{lx} = (g_l g_x/2)(1/\delta_l + 1/\delta_x)$, $\Delta_{lx} = \delta_l - \delta_x = \omega_{eg} + \omega_{c_x} - \omega_{c_l}$. In Eq. (4), the terms in the first two lines describe the photon-number-dependent stark shifts of the energy levels $|g\rangle$, $|e\rangle$, and $|f\rangle$, while the terms in the last line describe the $|g\rangle \leftrightarrow |e\rangle$ coupling caused due to the cooperation of cavities l and x. When $\Delta_{lx} \gg \{\lambda_l, \lambda_x, \lambda_{lx}\}$, the effective

Hamiltonian $H_{\rm e}$ turns into Refs. [36–38]

$$\begin{aligned} H_{\rm e} = & \sum_{l=1}^{N}(-\lambda_l\widehat{n}_l|g\rangle\langle g| + \lambda_l(1+\widehat{n}_l)|f\rangle\langle f|) - \lambda_x\widehat{n}_x|e\rangle\langle e| \\ & + \lambda_x(1+\widehat{n}_x)|f\rangle\langle f| - \sum_{l=1}^{n}\chi_{lx}\widehat{n}_l(1+\widehat{n}_x)|g\rangle\langle g| \\ & + \sum_{l=1}^{N}\chi_{lx}(1+\widehat{n}_l)\widehat{n}_x|e\rangle\langle e|, \end{aligned} \tag{5}$$

where $\chi_{lx} = \lambda_{lx}^2/\Delta_{lx}$. In the case of the levels $|e\rangle$ and $|f\rangle$ being initially not occupied, these levels will not be populated because neither $|g\rangle \leftrightarrow |e\rangle$ transition nor $|g\rangle \leftrightarrow |f\rangle$ transition is induced by Hamiltonian (5). Therefore, Hamiltonian (5) reduces to

$$H_{\rm e} = -\sum_{l=1}^{N}\lambda_l\widehat{n}_l|g\rangle\langle g| - \sum_{l=1}^{N}\chi_{lx}\widehat{n}_l(1+\widehat{n}_x)|g\rangle\langle g|. \tag{6}$$

In the following, we assume that the qutrit is initially in the ground state $|g\rangle$. Note that the qutrit will remain in this state because none of interlevel transitions of the qutrit can be induced by Hamiltonian (6). Hamiltonian (6) thus reduces to

$$\widetilde{H}_{\rm e} = -\sum_{l=1}^{N}\eta_l\widehat{n}_l - \sum_{l=1}^{N}\chi_{lx}\widehat{n}_l\widehat{n}_x, \tag{7}$$

where $\eta_l = \lambda_l + \chi_{lx}$. The effective Hamiltonian $\widetilde{H}_{\rm e}$ characterizes the dynamics of the cavity system. Under this Hamiltonian, the unitary operator $U = e^{-i\widetilde{H}_{\rm e}t}$ describing the state time evolution of the cavity system can be expressed as

$$U = \prod_{l=1}^{N}U_{lx} \otimes \prod_{l=1}^{N}U_l, \tag{8}$$

with

$$U_{lx} = \exp(i\chi_{lx}\widehat{n}_l\widehat{n}_x t), \quad U_l = \exp(i\eta_l\widehat{n}_l t), \tag{9}$$

where U_l is a unitary operator on cavity l, while U_{lx} is a unitary operator on cavities x and l ($l = 1, 2, \ldots, N$). Under the following two conditions

$$\eta_l t = 2\pi s_l, \quad \chi_{lx}t = \frac{\pi}{N}, \tag{10}$$

where s_l is a positive integer for cavity l and N is the total number of control qubits, the unitary operator U of the cavity system can be finally expressed as

$$U = \exp\left(i\frac{\pi}{N}\widehat{n}_x\sum_{l=1}^{N}\widehat{n}_l\right). \tag{11}$$

For $N+1$ photonic qubits, target qubit x and control qubit l ($l = 1, 2, \ldots, N$), we consider the initial state of the cavity system $|n_1, n_2, \ldots, n_N, n_x\rangle_m$ ($n_1, n_2, n_3, \ldots, n_N, n_x \in \{0, 1\}$), where subscript m is the number of the control qubits in the state $|1\rangle$. After the unitary operator U (given in Eq. 11), it is straightforward to get the following state transformation:

$$\begin{aligned} & U|n_1, n_2, \ldots, n_N, 0\rangle_m = |n_1, n_2, \ldots, n_N, 0\rangle_m, \\ & U|n_1, n_2, \ldots, n_N, 1\rangle_m = e^{i\frac{m\pi}{N}}|n_1, n_2, \ldots, n_N, 1\rangle_m, \end{aligned} \tag{12}$$

which implies that if the target qubit x is in the state $|0\rangle$, the state of the cavity system remains unchanged; yet, if the target qubit x is in the state $|1\rangle$, the phase associated with m appears in the final state. When the target qubit x is in the quantum state $|+\rangle = (|0\rangle + |1\rangle)/\sqrt{2}$, after the vote, a relative phase related to m is introduced between the state $|0\rangle$ and the state $|1\rangle$ in the quantum state of the target qubit x. This phase can be obtained by performing Wigner tomography [39] on the target qubit.

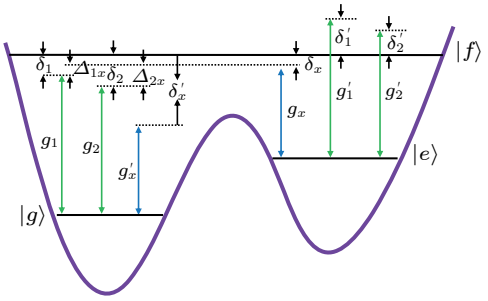

Fig. 3. Representation of the coupling between cavity 1 and the $|g\rangle \leftrightarrow |f\rangle$ transition of the qutrit (with coupling constant g_1 and detuning δ_1), the coupling between cavity 2 and the $|g\rangle \leftrightarrow |f\rangle$ transition of the qutrit (with coupling constant g_2 and detuning δ_2), and the coupling between cavity x and the $|e\rangle \leftrightarrow |f\rangle$ transition of the qutrit (with coupling constant g_x and detuning δ_x). Furthermore, depiction of the unwanted coupling between cavity 1 and the $|e\rangle \leftrightarrow |f\rangle$ transition of the qutrit (with coupling constant g_1' and detuning δ_1'), the unwanted coupling between cavity 2 and the $|e\rangle \leftrightarrow |f\rangle$ transition of the qutrit (with coupling constant g_2' and detuning δ_2'), as well as the unwanted coupling between cavity x and the $|g\rangle \leftrightarrow |f\rangle$ transition of the qutrit (with coupling constant g_x' and detuning δ_x'). Note that the coupling of each cavity with the $|g\rangle \leftrightarrow |e\rangle$ transition of the qutrit is negligible due to the weak $|g\rangle \leftrightarrow |e\rangle$ transition.

As an example, we investigate the experimental feasibility for the simple 2-voter QVM by using three one-dimensional microwave cavities coupled to an SC flux qutrit. The initial state of the whole system is

$$|\psi(0)\rangle = |n_1, n_2, +\rangle \otimes |g\rangle, \quad (n_1,\, n_2 \in \{0,\, 1\}), \tag{13}$$

where $|g\rangle$ is the ground state of the qutrit A, and $|+\rangle = (|0\rangle + |1\rangle)/\sqrt{2}$ is the state of cavity x, which is the equal probability superposition of the vacuum state $|0\rangle$ and the single-photon sate $|1\rangle$. After applying the unitary operator U of Eq. (11) with two control qubits ($N = 2$), the initial state changes to

$$|\psi(T)\rangle = |n_1, n_2\rangle \otimes \frac{1}{\sqrt{2}}(|0\rangle + e^{i\frac{m\pi}{2}}|1\rangle) \otimes |g\rangle, \ (n_1,\, n_2 \in \{0,\, 1\}), \tag{14}$$

where only a phase $m\pi/2$ ($m = n_1 + n_2$) associated with two control qubits is attached to the state $|1\rangle$ of the target qubits, while the state $|0\rangle$ of the target qubit remains unchanged.

The Hamiltonian used for the generation of $|\psi(T)\rangle$ is the effective Hamiltonian (7) with $N = 2$. This Hamiltonian was derived from the original Hamiltonian (2) with

$N = 2$, which only includes the coupling between cavity l ($l = 1, 2$) and the $|g\rangle \leftrightarrow |f\rangle$ transition as well as the coupling between cavity x and the $|e\rangle \leftrightarrow |f\rangle$ transition of the SC flux qutrit. In a realistic situation as shown in Fig. 3, there are the unwanted coupling between cavity l ($l = 1, 2$) and the $|e\rangle \leftrightarrow |f\rangle$ transition as well as the unwanted coupling between cavity x and the $|g\rangle \leftrightarrow |f\rangle$ transition of the SC flux qutrit. Moreover, there is the unwanted intercavity crosstalk between the three cavities. When the unwanted couplings and the unwanted intercavity crosstalk are taken into account, Hamiltonian (2), with $N = 2$ for the present case, is modified as

$$\begin{aligned} H_{I_0} = & \sum_{l=1}^{2}(g_l e^{-i\delta_l t}\hat{a}_l^+\delta_{fg}^- + \text{H.c.}) + g_x e^{-i\delta_x t}\hat{a}_x^+\delta_{fe}^- + \text{H.c.} \\ & + \sum_{l=1}^{2}(g_l' e^{-i\delta_l' t}\hat{a}_l^+\delta_{fe}^- + \text{H.c.}) + g_x' e^{-i\delta_x' t}\hat{a}_x^+\delta_{fg}^- + \text{H.c.} \\ & + (\widetilde{g}_{12}e^{-i\widetilde{\Delta}_{12}t}\hat{a}_1^+\hat{a}_2 + \widetilde{g}_{2x}e^{-i\widetilde{\Delta}_{2x}t}\hat{a}_2^+\hat{a}_x \\ & + \widetilde{g}_{1x}e^{-i\widetilde{\Delta}_{1x}t}\hat{a}_1^+\hat{a}_x + \text{H.c.}), \end{aligned} \tag{15}$$

where the terms in the first line is the ideal Hamiltonian (2) with $N = 2$, the first term in the second line represents the unwanted coupling between cavity l ($l = 1, 2$) and the $|e\rangle \leftrightarrow |f\rangle$ transition of the SC qutrit with coupling constant g_l' and detuning $\delta_l' = \omega_{fe} - \omega_{c_l}$, the second term in the second line represents the unwanted coupling between cavity x and the $|g\rangle \leftrightarrow |f\rangle$ transition of the SC qutrit with coupling constant g_x' and detuning $\delta_l' = \omega_{fg} - \omega_{c_x}$, while the terms in the third and fourth lines represent the unwanted intercavity crosstalk among the three cavities, with $\tilde{g}_{ll'}$ ($\tilde{\Delta}_{ll'} = \omega_l - \omega_{l'}$) the crosstalk strength (the frequency detuning) between the two cavities l and l' ($l, l' = 1, 2, x; l \neq l'$). Because the $|g\rangle \leftrightarrow |e\rangle$ transition can be made weak by increasing the barrier between the two potential wells of the SC qutrit, the coupling of each cavity with the $|g\rangle \leftrightarrow |e\rangle$ transition of the SC qutrit is negligible and thus is not considered in the above Hamiltonian (15).

Taking into account finite qutrit relaxation, dephasing, and photon lifetime, the dynamics of the lossy system is governed by the following master equation:

$$\begin{aligned} \frac{d\rho}{dt} = & -i[H_{I_0}, \rho] + \sum_{j=1}^{3}\kappa_j\mathcal{L}[\hat{a}_j] \\ & + \gamma_{eg}\mathcal{L}[\sigma_{eg}^-] + \gamma_{fe}\mathcal{L}[\sigma_{fe}^-] + \gamma_{fg}\mathcal{L}[\sigma_{fg}^-] \\ & + \gamma_{e,\varphi}(\sigma_{ee}\rho\sigma_{ee} - \sigma_{ee}\rho/2 - \rho\sigma_{ee}/2) \\ & + \gamma_{f,\varphi}(\sigma_{ff}\rho\sigma_{ff} - \sigma_{ff}\rho/2 - \rho\sigma_{ff}/2), \end{aligned} \tag{16}$$

where $\mathcal{L}[\Lambda] = \Lambda\rho\Lambda^+ - \Lambda^+\Lambda\rho/2 - \rho\Lambda^+\Lambda/2$ ($\Lambda = \hat{a}_j, \sigma_{eg}^-, \sigma_{fe}^-, \sigma_{fg}^-$), $\sigma_{ee} = |e\rangle\langle e|$, $\sigma_{ff} = |f\rangle\langle f|$, γ_{eg} is the energy relaxation rate of the level $|e\rangle$ for the decay path $|e\rangle \to |g\rangle$, γ_{fe} (γ_{fg}) is the relaxation rate of the level $|f\rangle$ for the decay path $|f\rangle \to |e\rangle$ ($|f\rangle \to |g\rangle$), $\gamma_{e,\varphi}$ ($\gamma_{f,\varphi}$) is the dephasing rate of the level $|e\rangle$ ($|f\rangle$) of the qutrit, while κ_j is the decay rate of cavity j ($j = 1, 2, x$). We utilize the QUTIP [40] for numerical calculations, which is an open-source tool designed for simulating the dynamics of open quantum systems.

To measure the accuracy of the QVM, we evaluate the fidelity of the final state $|\psi(T_f)\rangle$ by

$$\mathcal{F} = \sqrt{\langle\psi_{\text{id}}|\rho|\psi_{\text{id}}\rangle}, \tag{17}$$

where $|\psi_{\text{id}}\rangle = |\psi(T_f)\rangle$ denotes the ideal final state. The ideal final state $|\psi_{\text{id}}\rangle$ is derived without considering in system dissipation, intercavity crosstalk, and unwanted couplings, whereas ρ represents the density operator characterizing the realistic final state of the system, which is achieved by numerically solving the master equation and considering the operation performed in a realistic situation.

Table 1. Parameters used in the numerical simulation.

$\omega_{ge}/2\pi = 8.0\,\text{GHz}$	$\omega_{ef}/2\pi = 12.0\,\text{GHz}$	$\omega_{gf}/2\pi = 20.0\,\text{GHz}$
$\omega_{c1}/2\pi = 19.159\,\text{GHz}$	$\omega_{c2}/2\pi = 19.120\,\text{GHz}$	$\omega_{cx}/2\pi = 11.208\,\text{GHz}$
$\delta_1/2\pi = 841\,\text{MHz}$	$\delta_2/2\pi = 880\,\text{MHz}$	$\delta_x/2\pi = 792\,\text{MHz}$
$\delta_1'/2\pi = -7.159\,\text{GHz}$	$\delta_2'/2\pi = -7.120\,\text{GHz}$	$\delta_x'/2\pi = 8.792\,\text{GHz}$
$\widetilde{\Delta}_{12}/2\pi = 39\,\text{MHz}$	$\widetilde{\Delta}_{1x}/2\pi = 7.951\,\text{GHz}$	$\widetilde{\Delta}_{2x}/2\pi = 7.912\,\text{GHz}$
$g_1/2\pi = 21.4\,\text{MHz}$	$g_2/2\pi = 29.4\,\text{MHz}$	$g_x/2\pi = 88\,\text{MHz}$
$g_1'/2\pi = 21.4\,\text{MHz}$	$g_2'/2\pi = 29.4\,\text{MHz}$	$g_x'/2\pi = 88\,\text{MHz}$
$g_{12}/2\pi = 0.88\,\text{MHz}$	$g_{1x}/2\pi = 0.88\,\text{MHz}$	$g_{2x}/2\pi = 0.88\,\text{MHz}$
$\kappa_1 = \kappa_2 = \kappa_x = \kappa$	$\gamma_{fe}^{-1} = T$	$\gamma_{fg}^{-1} = T$
$\gamma_{eg}^{-1} = 10T$	$\gamma_{\phi e}^{-1} = T/2$	$\gamma_{\phi f}^{-1} = T/2$

Table 1 lists the parameters used in the numerical simulations. By a proper design of the flux qutrit,[41] one can have $\phi_{fg} \sim \phi_{fe} \sim 10\phi_{eg}$, where ϕ_{ij} is the dipole coupling matrix element between the two levels $|i\rangle$ and $|j\rangle$ with $ij \in \{eg, fe, fg\}$. Thus, one has $g_1' \sim g_1$, $g_2' \sim g_2$ and $g_x' \sim g_x$, while the $|g\rangle \leftrightarrow |e\rangle$ transition is much weaker compared to the $|g\rangle \leftrightarrow |f\rangle$ and $|e\rangle \leftrightarrow |f\rangle$ transitions of the qutrit. Other parameters used in the numerical simulations are as follows: (i) $\gamma_{eg}^{-1} = 10T$, $\gamma_{fe}^{-1} = T$, $\gamma_{fg}^{-1} = T$, $\gamma_{\phi e}^{-1} = \gamma_{\phi f}^{-1} = T/2$, (ii) $\kappa_1 = \kappa_2 = \kappa_3 = \kappa$, (iii) $g_{12} = g_{2x} = g_{1x} = g_{cr}$. We should mention that γ_{eg}^{-1} is much larger than γ_{fe}^{-1} and γ_{fg}^{-1} because of $\phi_{fg} \sim \phi_{fe} \sim 10\phi_{eg}$. The value of T adopted in our numerical simulations is 3–10 μs. Hence, the decoherence time of the qutrit used

in the numerical simulations ranges from 30 to 100 μs. It is a rather conservative consideration, as experimental evidence has demonstrated decoherence times of 70 μs to 1 ms for SC flux devices.[12,42]

By numerically solving the master equation (16), we plot Fig. 4 to present the fidelity versus κ^{-1} for $T = 3\,\mu s$ (red rhombus), 5 μs (blue pentagon), 10 μs (green square), $g_{cr} = 0.01\ \max\{g_1, g_2, g_x\}$ and s_1 $(s_2) = 1$ (2), for Eq. (10). Figure 4(a) shows the situation where two voters cast negative votes with an initial state $|00, +\rangle$. Obviously, for this initial state, the photon number in the two cavities of the control qubits is 0. The fidelity is thus less affected by the cavity dissipation compared to Figs. 4(b), 4(c), and 4(d). Furthermore, Fig. 4(a) shows that the fidelity is also only slightly influenced by changes in T. Figures 4(b) and 4(c) show the situation where two voters cast only one affirmative vote with initial state $|01, +\rangle$ and $|10, +\rangle$. In these two cases, the photon number only in one of the two cavities (control qubits), and the fidelity is significantly more affected by the cavity dissipation compared to Fig. 4(a). Additionally, Figs. 4(b) and 4(c) demonstrate that the fidelity increases as T increases. Figure 4(d) shows the situation where both voters cast affirmative votes with an initial state $|11, +\rangle$. The photon number in either of the two cavities (control qubits) is 1. The effect of the cavity dissipation is significantly greater than that in other cases. For example, at $T = 3\,\mu s$ and $\kappa^{-1} = 40\,\mu s$, the fidelity in the case of Fig. 4(d) is lower than 93%, while the fidelity in the cases of Figs. 4(b) and 4(c) is higher than 95.5%, and it is even higher than 99% in the case of Fig. 4(a).

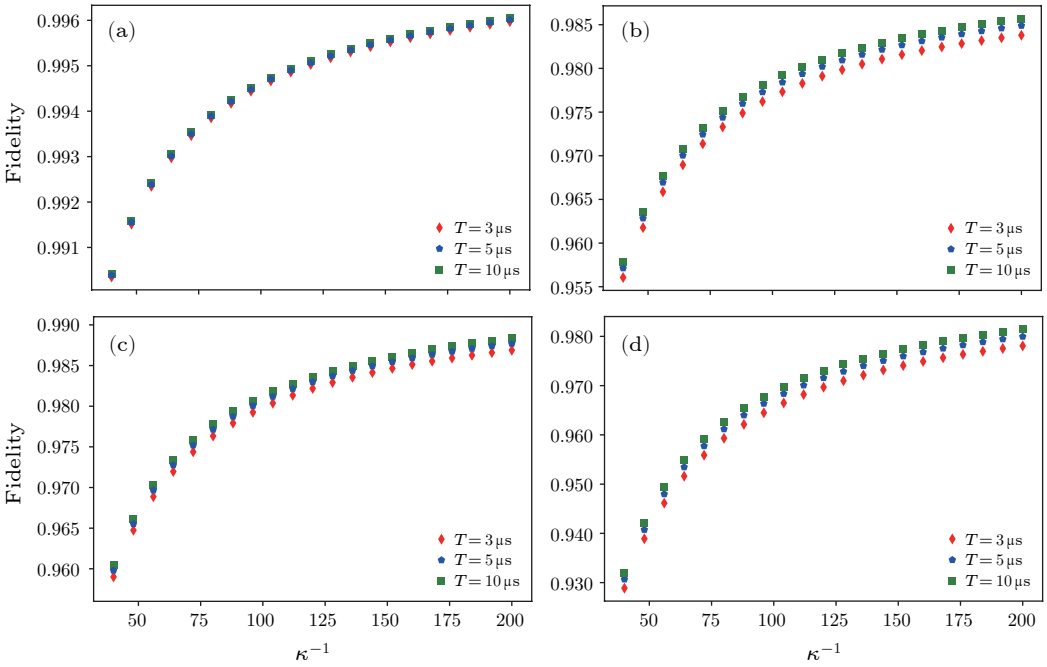

Fig. 4. Fidelity versus κ^{-1} for $T = 3$, 5, and 10 μs: (a) the situation where two voters cast negative votes with an initial state $|00, +\rangle$, (b) the situation where two voters cast only one affirmative vote with an initial state $|01, +\rangle$, (c) the situation where two voters cast only one affirmative vote with an initial state $|10, +\rangle$, (d) the situation where both voters cast affirmative votes with an initial state $|11, +\rangle$.

In summary, we have proposed a scheme for implementing a QVM based on the microwave photonic qubit encoding. In this scheme, the QVM primarily operates the voting process through a multi-control single-target quantum phase gate. Due to the fact that the voting result is only related to the total number of affirmative votes, and thus incapable of reflecting specific voting information of each voter, anonymity is thereby ensured. As we can obtain the phase information on the single-target qubit via the Wigner function tomography method, the verifiability of the voting result is ensured. Furthermore, our QVM has scalability in terms of the number of voters and is general in its physical implementation, meaning that it is not limited to circuit QED in physical implementation. As long as the multi-control single-target quantum phase gate in our scheme can be realized in other physical systems, the QVM can be implemented. In addition, our scheme involves a simple operation process, requiring only a single-step operation and the reading of a single target qubit. Finally, numerical calculations indicate that even under conservative parameter conditions, our proposed QVM scheme demonstrates a certain feasibility with the current quantum technology.

Acknowledgments. This work was partly supported by the National Natural Science Foundation of China (Grant Nos. 12074179 and U21A20436), the Innovation Program for Quantum Science and Technology (Grant No. 2021ZD0301702), the Natural Science Foundation of

Jiangsu Province, China (Grant Nos. BE2021015-1 and BK20232002), the Jiangsu Funding Program for Excellent Postdoctoral Talent (Grant No. 20220ZB16), and the Natural Science Foundation of Shandong Province, China (Grant No. ZR2023LZH002).

References

[1] Li Y R, Jiang D H, Zhang Y H, and Liang X Q 2021 *Quantum Inf. Process.* **20** 110
[2] Xu L and Wang M 2022 *Front. Phys.* **10** 1023992
[3] Jiang D H, Wang J, Liang X Q, Xu G B, and Qi H F 2020 *Int. J. Theor. Phys.* **59** 436
[4] Xue P and Zhang X 2017 *Sci. Rep.* **7** 7586
[5] Shi R H, Qin J Q, Liu B, and Zhang M W 2021 *Eur. Phys. J. D* **75** 20
[6] Yang C P, Chu S I, and Han S 2003 *Phys. Rev. A* **67** 042311
[7] Xiang Z L, Ashhab S, You J Q, and Nori F 2013 *Rev. Mod. Phys.* **85** 623
[8] Li J W, Wu C W, and Dai H Y 2011 *Chin. Phys. Lett.* **28** 090302
[9] Wang Z, Bao Z, Wu Y, Li Y, Ma C, Cai T, Song Y, Zhang H, and Duan L 2021 *Chin. Phys. Lett.* **38** 110303
[10] Place A P M, Rodgers L V, Mundada P, Smitham B M, Fitzpatrick M, Leng Z Q, Premkumar A, Bryon J, Vrajitoarea A, Sussman S *et al.* 2021 *Nat. Commun.* **12** 1779
[11] Wang C L, Li X G, Xu H K, Li Z Y, Wang J H, Yang Z, Mi Z Y, Liang X H, Su T, Yang C H *et al.* 2022 *npj Quantum Inf.* **8** 3
[12] Yan F, Gustavsson S, Kamal A, Birenbaum J, Sears A P, Hover D, Gudmundsen T J, Rosenberg D, Samach G, Weber S *et al.* 2016 *Nat. Commun.* **7** 12964
[13] Somoroff A, Ficheux Q, Mencia R A, Xiong H, Kuzmin R, and Manucharyan V E 2023 *Phys. Rev. Lett.* **130** 267001
[14] Chen W, Bennett D A, Patel V, and Lukens J E 2008 *Supercond. Sci. Technol.* **21** 075013
[15] Leek P J, Baur M, Fink J M, Bianchetti R, Steffen L, Filipp S, and Wallraff A 2010 *Phys. Rev. Lett.* **104** 100504
[16] Megrant A, Neill C, Barends R, Chiaro B, Chen Y, Feigl L, Kelly J, Lucero E, Mariantoni M, O'Malley P J J *et al.* 2012 *Appl. Phys. Lett.* **100** 113510
[17] Calusine G, Melville A, Woods W, Das R, Stull C, Bolkhovsky V, Braje D, Hover D, Kim D K, Miloshi X *et al.* 2018 *Appl. Phys. Lett.* **112** 062601
[18] Woods W, Calusine G, Melville A, Sevi A, Golden E, Kim D K, Rosenberg D, Yoder J L, and Oliver W D 2019 *Phys. Rev. Appl.* **12** 014012
[19] Melville A, Calusine G, Woods W, Serniak K, Golden E, Niedzielski B M, Kim D K, Sevi A, Yoder J L, Dauler E A *et al.* 2020 *Appl. Phys. Lett.* **117** 124004
[20] Reagor M, Pfaff W, Axline C, Heeres R W, Ofek N, Sliwa K, Holland E, Wang C, Blumoff J, Chou K *et al.* 2016 *Phys. Rev. B* **94** 014506
[21] Kudra M, Biznárová J, Fadavi Roudsari A, Burnett J J, Niepce D, Gasparinetti S, Wickman B, and Delsing P 2020 *Appl. Phys. Lett.* **117** 070601
[22] Romanenko A, Pilipenko R, Zorzetti S, Frolov D, Awida M, Belomestnykh S, Posen S, and Grassellino A 2020 *Phys. Rev. Appl.* **13** 034032
[23] Devoret M H and Schoelkopf R J 2013 *Science* **339** 1169
[24] Zhang G Q, Feng W, Xiong W, Xu D, Su Q P, and Yang C P 2023 *Phys. Rev. Appl.* **20** 044014
[25] Liu T, Zhou Y H, Wu Q C, and Yang C P 2022 *Appl. Phys. Lett.* **121** 244001
[26] Zhang Y, Zhao X, Zheng Z F, Yu L, Su Q P, and Yang C P 2017 *Phys. Rev. A* **96** 052317
[27] Puri S, St-Jean L, Gross J A, Grimm A, Frattini N E, Iyer P S, Krishna A, Touzard S, Jiang L, Blais A *et al.* 2020 *Sci. Adv.* **6** eaay5901
[28] Xu Q, Iverson J K, Brandão F G S L, and Jiang L 2022 *Phys. Rev. Res.* **4** 013082
[29] Kang Y H, Chen Y H, Wang X, Song J, Xia Y, Miranowicz A, Zheng S B, and Nori F 2022 *Phys. Rev. Res.* **4** 013233
[30] Chen Y H, Stassi R, Qin W, Miranowicz A, and Nori F 2022 *Phys. Rev. Appl.* **18** 024076
[31] Krasnok A, Dhakal P, Fedorov A, Frigola P, Kelly M, and Kutsaev S 2024 *Appl. Phys. Rev.* **11** 011302
[32] Pietikäinen I, Černotík O, Eickbusch A, Maiti A, Garmon J W, Filip R, and Girvin S M 2024 arXiv:2403.02278 [quant-ph]
[33] Neeley M, Ansmann M, Bialczak R C, Hofheinz M, Katz N, Lucero E, O'Connell A, Wang H, Cleland A N, and Martinis J M 2008 *Nat. Phys.* **4** 523
[34] Sun G, Wen X, Mao B, Chen J, Yu Y, Wu P, and Han S 2010 *Nat. Commun.* **1** 51
[35] Wang Z L, Zhong Y P, He L J, Wang H, Martinis J M, Cleland A N, and Xie Q W 2013 *Appl. Phys. Lett.* **102** 163503
[36] Zheng S B and Guo G C 2000 *Phys. Rev. Lett.* **85** 2392
[37] Sørensen A and Mølmer K 1999 *Phys. Rev. Lett.* **82** 1971
[38] James D F and Jerke J 2007 *Can. J. Phys.* **85** 625
[39] Shalibo Y, Resh R, Fogel O, Shwa D, Bialczak R, Martinis J M, and Katz N 2013 *Phys. Rev. Lett.* **110** 100404
[40] Johansson J R, Nation P D, and Nori F 2012 *Comput. Phys. Commun.* **183** 1760
[41] Liu Y x, You J Q, Wei L F, Sun C P, and Nori F 2005 *Phys. Rev. Lett.* **95** 087001
[42] You J Q, Hu X D, Ashhab S, and Nori F 2007 *Phys. Rev. B* **75** 140515